Decreasing Spatial Variability of Individual Watershed Areas by Revascularization Therapy in Patients With High-Grade Carotid Artery Stenosis

Lena Schmitzer,[1,2*] Nico Sollmann, MD, PhD,[1,2,3] Jan Kufer,[1,2] Michael Kallmayer, MD,[4] Hans-Henning Eckstein, MD,[4] Claus Zimmer, MD,[1,2] Christine Preibisch, PhD,[1,2,5] Stephan Kaczmarz,[1,2] and Jens Göttler, MD[1,2]

Background: Carotid artery stenosis can impair cerebral hemodynamics especially within watershed areas (WSAs) between vascular territories. WSAs can shift because of collateral flow, which may be an indicator for increased hemodynamic implications and hence higher risk for ischemic stroke. However, whether revascularization treatment can reverse the spatial displacement of individual WSAs (iWSAs) and impaired hemodynamics remains unknown.
Hypothesis: That iWSAs spatially normalize because of hemodynamic improvement resulting from revascularization treatment.
Study Type: Prospective.
Population: Sixteen patients with unilateral, high-grade carotid artery stenosis confirmed by duplex ultrasonography and 17 healthy controls.
Field strength/Sequences: A 3 T-magnetization-prepared rapid acquisition gradient echo (MPRAGE), gradient-echo echo planar dynamic susceptibility contrast (DSC), and fluid-attenuated inversion recovery (FLAIR) sequences. Additionally, contrast-enhanced 3D gradient echo magnetic resonance angiography (MRA) and diffusion-tensor imaging (DTI) spin-echo echo planar imaging were performed.
Assessment: iWSAs were delineated by a recently proposed procedure based on time-to-peak maps from DSC perfusion MRI, which were also used to evaluate perfusion delay. We spatially compared iWSAs and perfusion delay before and after treatment (endarterectomy or stenting). Additionally, the Circle of Willis collateralization status was evaluated, and basic cognitive testing was conducted.
Statistical Tests: Statistical tests included two-sample t-tests and Chi-squared tests. A P value < 0.05 was considered to be statistically significant.
Results: After revascularization, patients showed a significant spatial shift of iWSAs and significantly reduced perfusion delay ipsilateral to the stenosis. Spatial shift of iWSA ($P = 0.007$) and cognitive improvement ($P = 0.013$) were more pronounced in patients with poor pre-existing collateralization.
Controls demonstrated stable spatial extent of iWSAs ($P = 0.437$) and symmetric perfusion delays between hemispheres over time ($P = 0.773$).
Data Conclusion: These results demonstrate the normalization of iWSA and impaired hemodynamics after revascularization in patients with high-grade carotid artery stenosis.
Level of Evidence: 2
Technical Efficacy: Stage 2

J. MAGN. RESON. IMAGING 2021.

View this article online at wileyonlinelibrary.com. DOI: 10.1002/jmri.27788

Received Mar 16, 2021, Accepted for publication Jun 4, 2021.

*Address reprint requests to: L.S., Ismaninger Straße 22, 81675 München, Germany.
E-mail: l.schmitzer@tum.de

From the [1]Department of Diagnostic and Interventional Neuroradiology, School of Medicine, Technical University of Munich (TUM), Germany; [2]TUM-Neuroimaging Center, School of Medicine, Technical University of Munich (TUM), Germany; [3]Department of Diagnostic and Interventional Radiology, University Hospital Ulm, Ulm, Germany; [4]Department for Vascular and Endovascular Surgery, School of Medicine, Technical University of Munich (TUM), Germany; and [5]Department of Neurology, School of Medicine, Technical University of Munich (TUM), Germany

Although approximately 10% of all ischemic strokes are caused by a stenosis of the internal carotid artery (ICA),[1,2] most patients, even those with high-grade ICA stenosis (ICAS), do not show any signs of transient or permanent cerebral ischemia, i.e., are clinically "asymptomatic".[3] The term "asymptomatic" however neglects that many of these patients have subtle cognitive impairments,[4] which often show a progressive increase up to symptoms comparable with those in severe dementia.[5,6] In such patients, chronic hemodynamic alterations have been found, which are pronounced within watershed areas (WSAs),[7,8] and may impact brain function even without evidence of stroke.[9]

Cerebral WSAs are located along the borders of the vascular territories of the brain's major cerebral arteries and are usually divided into external and internal WSAs. External WSAs can be found between the cortical territories of the anterior, middle, and posterior cerebral arteries (ACA, MCA, and PCA, respectively).[1] Internal WSAs are located in the white matter (WM) between the penetrating branches of the MCA and the superficial perfusion of the major vascular territories.[2] Because of their distal location in the vascular territories, WSAs become prone to chronic hypoperfusion and ischemic events due to reduced perfusion pressure resulting from ICAS.[10,11]

Although WSAs are essential for the clinical evaluation of hemodynamic infarction and chronic hemodynamic changes,[10,11] the identification of these regions remains challenging because of the variations in perfusion territories, that can be observed especially in patients with hemodynamic compromise due to increased collateral flow.[12,13] Recently, the increased spatial variability of WSAs was demonstrated in patients with asymptomatic, high-grade ICAS. Thus, an individual WSA (iWSA) segmentation approach has been proposed based on time-to-peak (TTP) maps from dynamic susceptibility contrast (DSC) magnetic resonance imaging (MRI).[14] As iWSA are located at the edges of vascular territories, TTP is delayed compared to more central regions in the territories of the main cerebral arteries even in normal hemodynamic conditions.[14] Therefore, TTP maps offer the possibility to spatially localize these regions based on perfusion delay patterns.

The revascularization treatment of the stenosis is known to significantly alter cerebral hemodynamics.[15] However, it remains unclear whether the higher spatial variability of iWSAs also decreases, which might indicate a reduced risk for stroke and cognitive decline. A normalization of the spatial localization and extent of iWSAs might therefore be a valuable biomarker for revascularization success and prognosis.

We hypothesized that iWSAs spatially normalize because of an improvement in perfusion after revascularization treatment.

MARTERIALS and Methods

Participants

The study was approved by the institutional review board of the clinic and was according to the Human Research Committee guidelines of the university. All participants provided written informed consent, and the study was conducted following the Declaration of Helsinki.

Sixteen patients (mean age at baseline scan 71.9 ± 6.1 years) with unilateral high-grade ICAS of the extracranial segment confirmed by duplex ultrasonography (>70% according to the NASCET criteria[16]) and 17 age-matched healthy controls (mean age at baseline scan 70.7 ± 5.4 years) were included in this prospective study (Table 1). In four patients, a mild or moderate ICAS was present contralaterally to the high-grade ICAS.

The examination of every participant included medical history, basic neurological examination, cognitive assessment, and MRI at two time points. The follow-up examination occurred at least 3 months after the baseline exam (mean follow-up time 14.6 ± 4.6 months; mean time between revascularization treatment and follow-up scan 7.3 ± 3.2 months). All ICAS patients received revascularization treatment after the first scan, which was either carotid endarterectomy (CEA; $n = 6$) or carotid artery stenting (CAS, $n = 10$). The individual treatment approach was based on individual clinical indication by the referring physicians. Healthy controls were re-scanned after a similar time interval between the two scans (mean time between scan 1 and 2 for controls/patients: 16.9 ± 2.0 months/12.2 ± 5.3 months). Exclusion criteria for enrollment in the study included a history of stroke, transitory ischemic attack, brain surgery, clinically remarkable structural MRI (eg, silent territorial ischemic lesions or bleedings) at baseline, severe chronic kidney disease, and general MRI contraindications. Patients were enrolled in the outpatient clinic of the Department for Vascular and Endovascular Surgery and healthy controls by word-of-mouth advertisement from May 2015 until May 2017. All subjects underwent cognitive testing by MMSE[17] during the baseline and follow-up examination.

Magnetic Resonance Imaging

Every subject underwent the same imaging protocol at both examinations on a clinical 3 T MRI scanner (Ingenia, Philips Healthcare, Best, The Netherlands) using a 16-channel head/neck coil. The imaging protocol included diffusion tensor imaging (DTI) and fluid-attenuated inversion recovery (FLAIR) sequences to screen for ischemic brain lesions and to evaluate WM hyperintensities (WMHs). Moreover, magnetization-prepared rapid acquisition gradient echo (MPRAGE) and DSC imaging were conducted to delineate iWSAs. Additionally, contrast-enhanced magnetic resonance angiography (MRA) was included in the imaging protocol,

TABLE 1. Clinical Characteristics

	Controls ($N = 17$)	Patients ($N = 16$)	P-value
Age (years)	70.7 ± 5.4	71.9 ± 6.1	0.564
Female *n* (%)	11 (65)	5 (31)	0.055
BMI mean ± std (kg/m^2)	27.9 ± 4.3	26.8 ± 5.5	0.535
Stenotic degree (% NASCET ± std)	n.a.	80.9 ± 0.1	n.a.
CAS *n* (%)	n.a.	10 (63)	n.a.
CEA *n* (%)	n.a.	6 (38)	n.a.
Fazekas score of WMH (mean ± std)			
Baseline	1.1 ± 0.9	1.6 ± 0.6	0.119
Follow-up	1.1 ± 0.9	1.6 ± 0.6	0.119
Hypertension n (%)	11 (64)	15 (93)	0.041*
Coronary heart disease n (%)	2 (12)	6 (38)	0.085
Peripheral artery occlusive disease *n* (%)	1 (6)	3 (19)	0.258
Diabetes *n* (%)	1 (6)	6 (38)	0.026*
Smoker *n* (%)	7 (41)	8 (50)	0.611
Packyears in smokers (mean ± std)	8.7 ± 13.6	15.9 ± 20.5	0.240
Aspirin *n* (%)	3 (18)	15 (93)	<0.001*
Antihypertensive treatment *n* (%)	9 (52)	13 (81)	0.085
Statins *n* (%)	4 (24)	10 (63)	0.024*
Antidiabetic treatment *n* (%)	1 (6)	4 (25)	0.126
MMSE (mean ± std)			
Baseline	28.6 ± 1.2	27.7 ± 2.7	0.222
Follow-up	29.4 ± 1.1	29.2 ± 0.8	0.689

BMI = body mass index, CAS = carotid artery stenting, CEA = carotid endarterectomy, MMSE = Mini-Mental State Examination, n.a. = not applicable, NASCET = North American Symptomatic Carotid Endarterectomy Trial, WMH = white matter hyperintensity.
Two-sample t-test for age, BMI, packyears, Fazekas score, and MMSE.
Chi-squared test for the remaining.
In the longitudinal comparison of MMSE within the patient and control group, respectively, none of the tests revealed statistically significant differences.
*Significant group difference ($P < 0.05$).

covering the brain-supplying arterial branches from the aortic arch up to the vertex. The sequence parameters were set as follows:

DTI: spin-echo echo planar imaging (EPI) with 32 gradient directions, b = 800 sec/mm^2, TR = 12.9 sec, TE = 61 msec, Half Fourier 0.7, SENSE 2, 60 slices, matrix 112 × 110, voxel size 2.0 × 2.0 × 2.0 mm^3, number of signal averages (NSA) 2, acquisition time 15:30 min.

FLAIR: TR = 4800 msec, TE = 289 msec, flip angle (α) = 90°, 163 slices covering the whole brain, field of view (FOV) 250 × 250 × 183 mm^3, acquisition voxel size 1.12 × 1.12 × 1.12 mm^3 (reconstructed voxel size 1.0 × 1.0 × 1.0 mm^3), turbo spin echo (TSE) factor 167, inversion delay 1650 msec, acquisition time 4:34 min.

MPRAGE: TI = 1000 msec, TR = 2300 msec, TE = 4 msec, flip angle (α) = 9°, SENSE AP/RL 1.5/2.0, 170 slices covering the whole brain, FOV 240 × 240 × 170 mm^3, voxel size 1.0 × 1.0 × 1.0 mm^3, acquisition time 5:59 min.

DSC data were obtained during a bolus injection of weight-adjusted Gd-DOTA (DOTAREM® 0.5 mmol/mL, Guerbet GmbH, Roissy, France, concentration, 0.5 mmol/mL;

dose, 0.1 mmol/kg, at least 7.5 mmol per subject; flow rate, 4 mL/sec; injection 7.5 sec after DSC imaging started) using a single-shot gradient echo EPI readout, TR = 1513 msec, TE = 30 msec, flip angle (α) = 60°, 80 repetitions, FOV 224 × 224 × 100 mm^3, voxel size 2 × 2 × 3.5 mm^3, NSA 1, 26 slices, acquisition time 2:01 minutes, following the ASFNR recommendations.[18]

MRA was performed before the DSC and also served as a prebolus: 3D gradient echo sequence, TR = 5700 msec, TE = 2.1 msec, flip angle (α) = 37°, Half Fourier 0.75, SENSE 2 matrix size 508 × 443 × 144 mm^3, voxel size 0.63 × 0.63 × 1 mm^3, 144 slices acquisition time 2:27 minutes.

Image Processing

DSC data were processed using previously developed MATLAB-based software (MATLAB R2016b, MathWorks, Natick, MA, USA).[19] Preprocessing included filtering using a 3-D Gaussian spatiotemporal filter kernel of 3 mm full width at half maximum (FWHM) and slice time correction using SPM12 (Wellcome Trust Centre for Neuroimaging, UCL, London, UK) with default parameters.[20] Slice time correction was performed to account for temporal acquisition delays between neighboring slices due to interleaved slice acquisition order. The time of the contrast agent bolus entering the brain (i.e. global bolus arrival time) was automatically determined from the average signal of all brain voxels. TTP was then calculated as the interval between global bolus arrival time and each voxel's peak signal loss. Individual MPRAGE images were spatially co-registered to the DSC data. TTP maps were smoothed using an isotropic Gaussian kernel of 6 mm FWHM.

For each participant and for each scan, we defined the iWSA semi-automatically on the basis of TTP maps according to a previously developed two-step procedure (Figure 1).[14] Initially, TTP maps were thresholded at the 90th percentile and manually adapted. The second step included the removal of intraventricular space, restrictions of iWSAs to match local TTP maxima (achieved by different TTP windows adjusted to the individual's TTP), and exclusion of the venous system.[14] In subjects with asymmetrically increased TTP in the anterior circulation, different TTP windows for each hemisphere were applied to obtain an appropriate contrast for all watershed and nonwatershed regions. Furthermore, TTP windows were manually adjusted to generally increased TTP in posterior circulation to be able to identify TTP increases in typical WSAs. For detailed segmentation instructions, see reference[14]. This procedure was conducted by three operators (J.G., 5 years of experience, S.K., 5 years of experience, and L.S., 2 years of experience in cerebrovascular research), who were strictly blinded to the group assignment (i.e. control or patient group). iWSAs of J.G. were used for all further analyses. iWSAs segmented by S.K. and L.S. were used to assess inter-rater reliability (see below).

Data Analysis

All iWSAs from patients with left-sided ICAS were flipped along the mid-sagittal plane so that all hemispheres ipsilateral to the stenosis were located on the same side (i.e. the right side). Furthermore, maps were normalized to the Montreal Neurological Institute (MNI) standard space using SPM12. The dice coefficient (DC; $(A,B) = (2|A \cap B|) / (|A| + |B|)$, with A and B being the watershed masks of scans 1 and 2, respectively) was calculated for each subject's iWSA as derived from the baseline and follow-up scan. Additionally, the DC was used to assess interrater variability of iWSA segmentation by spatial comparison of iWSAs segmented by S. K. and L.S. to iWSAs segmented by J.G.

A probability map was calculated of all controls' iWSAs at baseline and follow-up, which displays the likelihood of a voxel being defined as part of an iWSA and therefore represents the mean location of the iWSAs in healthy controls. The probability map was thresholded at a likelihood of 80% and compared with each patient's whole iWSA as well as the iWSA of each side at both scan times using the DC to detect a possible normalization of patients' iWSAs in response to the revascularization treatment. The threshold was applied to restrict the volume of the probability map to the size of the participant's iWSAs.

To investigate hemodynamic changes after treatment, TTP values were normalized by the mean individual TTP in WM to obtain a relative TTP (rTTP) and extracted within each iWSA of the baseline and follow-up scan. rTTP values within each iWSA were analyzed separately for each hemisphere and scan.

FLAIR images were compared between both scans for all subjects by three raters (J.G., N.S., L.S.) to reveal new infarcts or postischemic lesions. Furthermore, the same rater determined the Fazekas score[21] of each participant in both scans to compare WMHs in both groups and to evaluate WMH changes that occurred in the interscan interval. Interrater agreement between the three readers regarding assignment of Fazekas scores was assessed using Fleiss' kappa.

Collateralization status was defined based on the configuration of the Circle of Willis (CoW) in the MRA in the baseline scan using a binary rating scale: a complete CoW (i.e. patent anterior communication artery and both posterior communicating arteries) was determined as an indicator of good collateral flow while an incomplete CoW (i.e. at least one atretic anterior or posterior communicating artery) was determined as poor collateral flow. These groups were used in a subgroup analysis to compare patients with good collateralization status ($n = 11$) to those with poor collateralization status ($n = 5$).

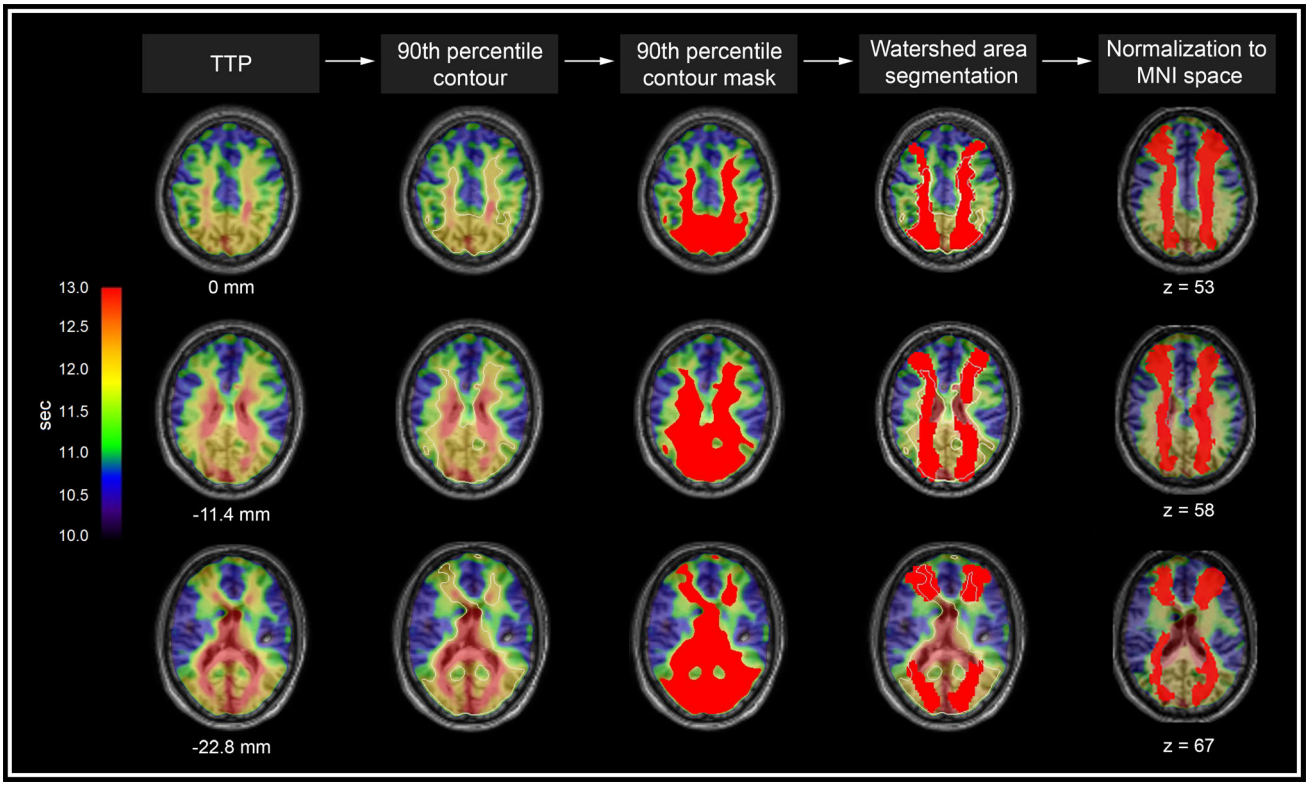

FIGURE 1: Overview of processing steps. Time-to-peak (TTP) maps derived from dynamic susceptibility contrast imaging were used for the definition of individual watershed areas (iWSAs) according to reference 14, which is illustrated in columns 1–5. Column 1: TTP map overlaid on MPRAGE data of a healthy control. High TTP is depicted in red, low TTP in blue (color bar). Columns 2 and 3: contouring of the 90th percentile of the whole brain histogram (white line) resulted in a preliminary 90th percentile mask (red overlay). Column 4: manual adaption of the initial 90th percentile mask was performed to include external/cortical watershed areas and to exclude mainly large vessels, the ventricular system, and choroid plexus. Column 5: afterward, iWSA masks were spatially normalized to MNI space.

Statistics

Subject characteristics were compared between groups by two-sample t-tests and Chi-squared tests. Two-sample t-tests were applied for group comparisons between baseline and follow-up scans regarding the DC and the Fazekas score, as well as for MMSE results. Inter-rater analysis of FLAIR lesions was assessed using Fleiss' kappa. Parameters were presented as mean ± standard deviation.

A *P*-value of ≤ 0.05 was considered statistically significant. SPSS (version 26.0; IBM SPSS Statistics for Windows, Armonk, NY, USA) was used for statistical analyses.

Results

All patients and controls who completed the follow-up scan were included in this study.

One patient showed a new lacunar lesion on the side of the revascularization treatment after CAS. The remaining patients and all healthy controls showed no new postischemic lesions in the follow-up compared with the baseline scan. The Fazekas score did not differ significantly between groups (mean score in baseline scan of controls/patients: 1.1/1.6, $P = 0.119$; Table 1) and remained identical between scans, indicating no substantial effects of ICAS and vascular interventions on WMH. The Fleiss' kappa with 0.79 reached substantial agreement.

iWSAs were reliably segmented in both groups (also see exemplary data in Figure 2) as assessed in an inter-rater reliability analysis in three operators. Here, we compared the spatial overlap of iWSA masks of two operators (S.K. and L.S.) to the third operator (J.G.) using the DC (scan 1: mean DC of iWSA by S.K./L.S.: 0.82 ± 0.11/0.81 ± 0.13; scan 2: S.K./L.S.: 0.95 ± 0.030/0.92 ± 0.03). In both ratings, no significant difference between the DC of the control and patient group was found in scan 1 (mean DC in controls/patients by S.K.: 0.84 ± 0.056/0.80 ± 0.15, $P = 0.26$ and by L.S. 0.82 ± 0.053/0.79 ± 0.14, $P = 0.34$) and scan 2 (mean DC in controls/patients by S.K.: 0.95 ± 0.031/0.96 ± 0.030, $P = 0.92$ and by L.S. 0.92 ± 0.027/0.93 ± 0.028, $P = 0.68$). These results demonstrate good inter-rater agreement and support the reliability of the used iWSA segmentation approach.

Spatial correspondence of iWSAs across scans was higher in the control group than in the patient group with a strong tendency toward statistical significance (mean DC of controls/patients: 0.621 ± 0.039/0.592 ± 0.047, $P = 0.069$; 95% confidence interval: − 0.0024, 0.060; Figure 3(a)).

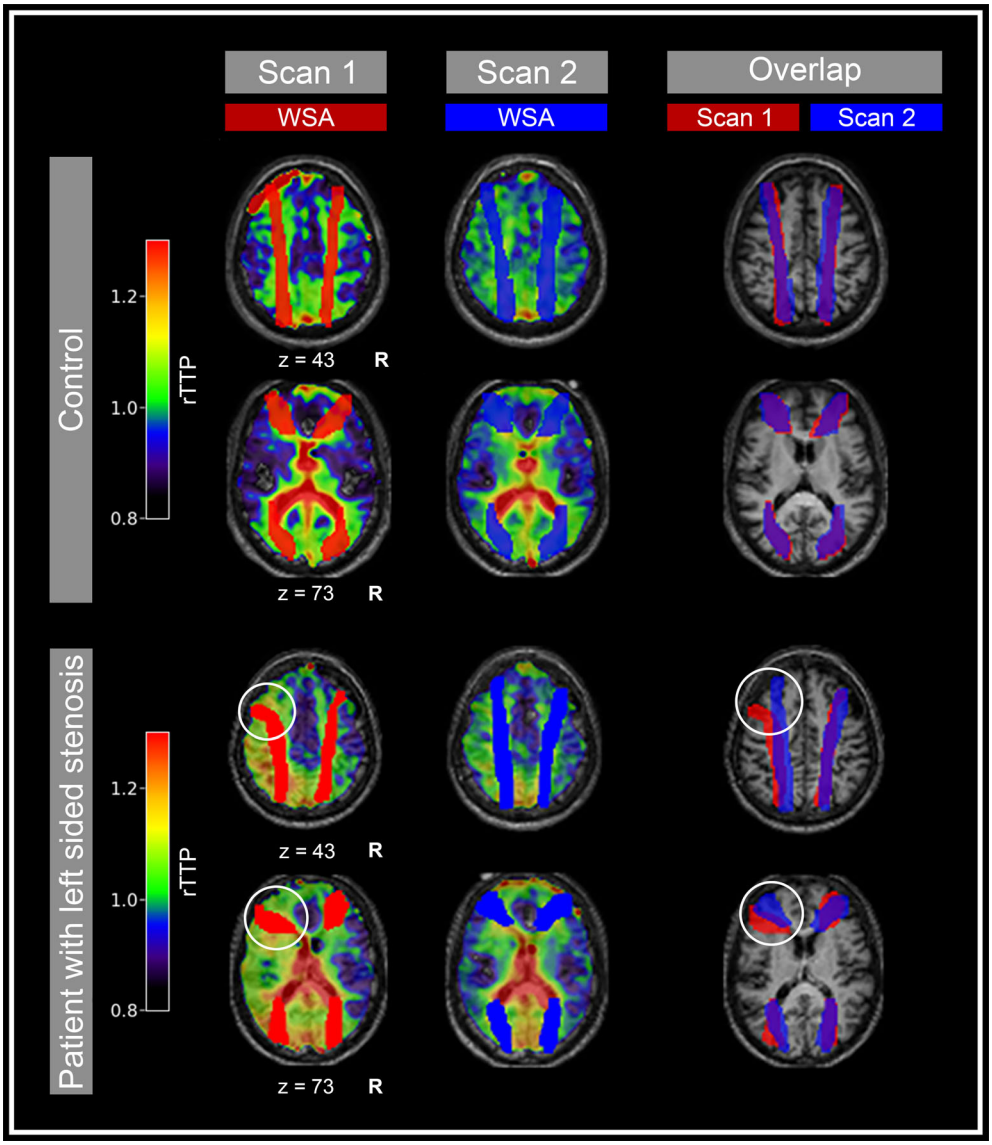

FIGURE 2: Example of individual watershed areas (iWSA) of baseline and follow-up scanning and their overlap. Exemplary data of a healthy control (upper two rows) and a patient with left-sided high-grade carotid artery stenosis (lower two rows) in MNI space. For better comparison of the baseline and follow-up scan, time-to-peak (TTP) maps were normalized to the mean TTP within white matter, resulting in relative TTP (rTTP) maps. Columns 1 and 2: color overlay of segmented iWSA of scan 1 (i.e. pre-interventional in patients) in red and scan 2 (i.e. postinterventional in patients) in blue. Column 3: Overlap of the iWSA of scan 1 and scan 2. Notice the incongruence of the patient's preinterventional and postinterventional iWSA in the hemisphere ipsilateral to the stenosis (circles).

When comparing spatial congruency of iWSAs in each hemisphere separately, patients' iWSAs on the side of the stenosis had significantly lower spatial correspondence than on the contralateral side (mean DC ipsilateral/contralateral to the stenosis: $0.589 \pm 0.067/0.634 \pm 0.037$; Figure 3(b)), indicating a shift of the iWSAs on the side of the revascularization treatment. Controls' iWSAs showed no significant spatial difference between the left and right hemisphere across scans (mean DC of left/right side: $0.617 \pm 0.033/0.628 \pm 0.044$, $P = 0.438$; Figure 3(b)).

The DC of the thresholded mean iWSA mask of controls and all patients' iWSAs was significantly higher after revascularization treatment than that in the baseline scan, however, did not significantly differ between the ipsilateral and contralateral side (mean DC of baseline/follow-up scan: $0.440 \pm 0.045/0.512 \pm 0.044$; Figure 3(c,d)).

In the baseline scan, rTTP values in the patients' hemisphere ipsilateral to the stenosis were significantly higher than in the contralateral side (mean rTTP in iWSA ipsilateral/contralateral to the stenosis: $1.103 \pm 0.083/1.050 \pm 0.069$; Figure 4(b,d), scan 1). In the patients with additional mild or moderate contralateral ICAS, asymmetrical rTTP increases were only observed on the side of the high-grade ICAS, thus we regard the high-grade ICAS as the leading cause for the

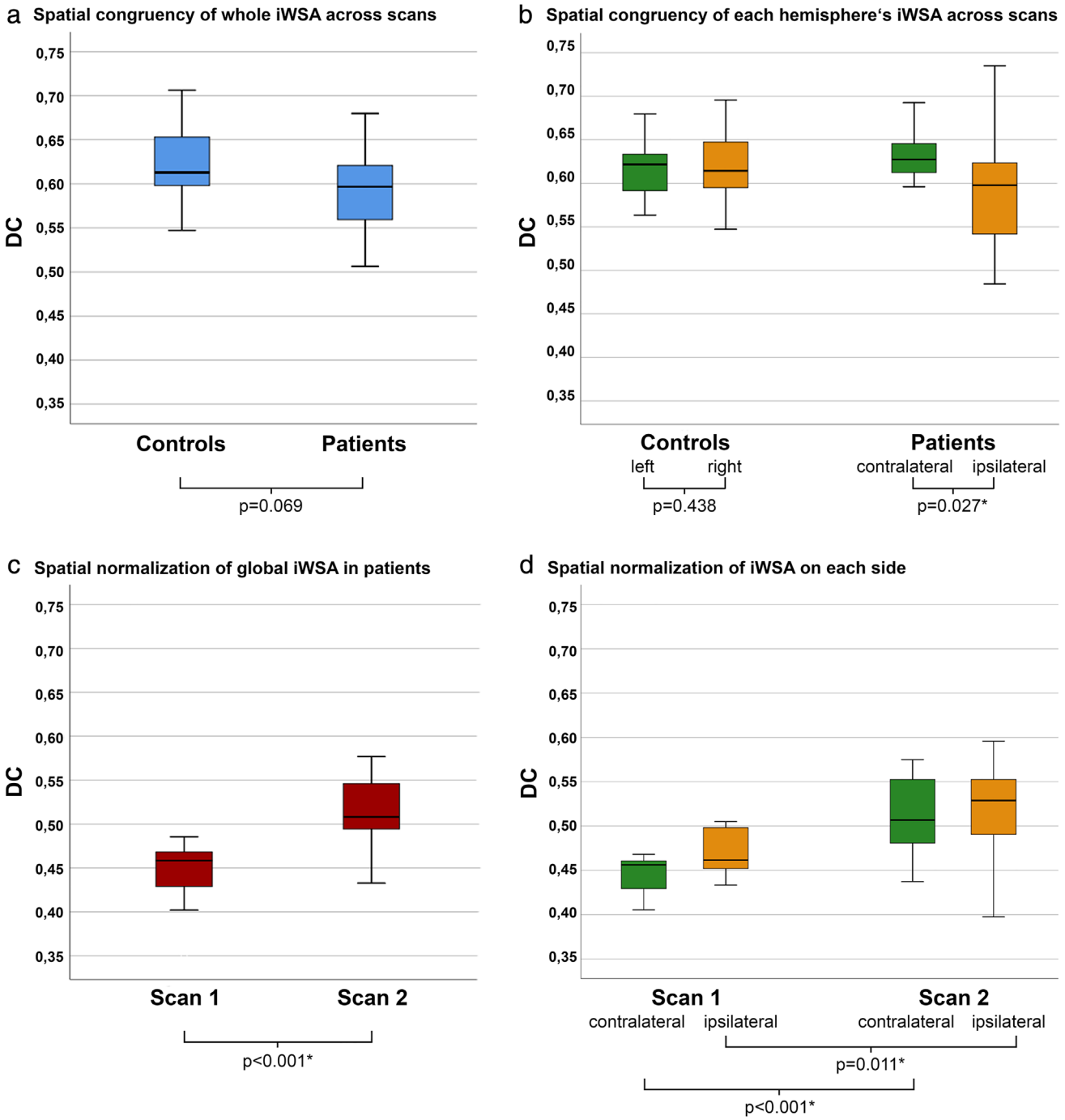

FIGURE 3: Spatial normalization of individual watershed areas (iWSAs) after carotid stenosis revascularization. (a) The dice coefficient (DC) was calculated for bilateral iWSAs between baseline and follow-up in each subject and compared between groups. Spatial correspondence between scans was higher in controls than in patients, tending toward statistical significance (median DC in controls/patients: 0.613/0.597, two-sample t-test: $P = 0.069$). (b) Spatial congruency of patient's iWSAs between baseline and follow-up scans in each hemisphere was significantly lower in the ipsilateral hemisphere than in the contralateral side (median DC patients ipsilateral/contralateral hemisphere: 0.598/0.632, two-sample t-test: $P = 0.027$), indicating a shift of iWSAs. Controls' iWSAs showed no significant difference (median DC controls left/right hemisphere: 0.619/0.620, two-sample t-test: $P = 0.438$). (c) Spatial congruency of patients' iWSAs with an averaged map of controls' iWSAs increased in the follow-up (scan 2) compared to baseline (scan 1) (median DC in scan 1/2: 0.458/0.508, two-sample t-test: $P < 0.001$). (d) Spatial comparison of patients' iWSA with the averaged WSA template of controls for each side. Significant increase of DCs on each side across the scans (median ipsilateral DC scan 1/2: $0.460 \pm 0.036/0.528 \pm 0.058$, $P = 0.011$, median contralateral DC scan 1/2: 0.455 ± 0.030 0.507 ± 0.041, $P < 0.001$). There was no significant side difference of DCs in scan 1 and 2 ($P > 0.05$). The boxes contain all single DC values between the first and third quartiles, the line inside marks the median, and the whiskers reach from minimum to maximum (not including outliers).

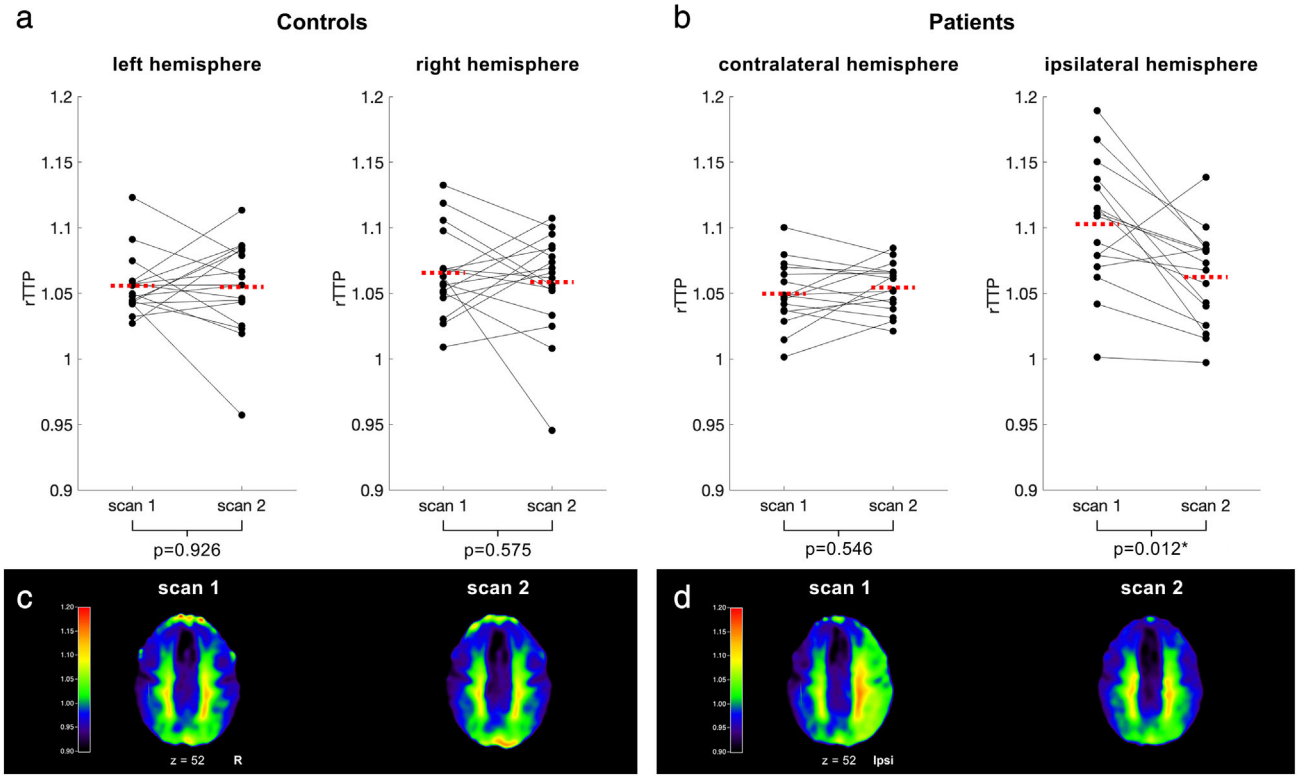

FIGURE 4: Comparison of relative time-to-peak (rTTP) values within individual watershed areas (iWSAs). Paired scatter plots depicting mean rTTP within iWSAs between (a) scan 1 vs. scan 2 in the right and left hemispheres in control subjects and (b) ipsilateral vs. contralateral to the stenosis in patients. Mean rTTP maps of controls and patients are displayed in (c) and (d), respectively. Before intervention, patients showed increased rTTP in the iWSAs ipsilateral to the stenosis (b, d) compared to the contralateral side. After revascularization treatment, rTTP values were reasonably symmetric between hemispheres. Controls had symmetrical and stable rTTP values in both hemispheres in both scans (a, c). The red dashed line indicates the mean rTTP values of the respective side.

hemodynamic changes. After revascularization treatment, rTTP symmetry was restored between hemispheres (mean rTTP in iWSA ipsilateral/contralateral to the stenosis: $1.062 \pm 0.058/1.054 \pm 0.056$, $P = 0.446$; Figure 4(b,d), scan 2). Controls' rTTP did not differ significantly between hemispheres in both scans (scan 1: left/right hemisphere: $1.056 \pm 0.063/1.066 \pm 0.066$, $P = 0.316$; scan 2: left/right hemisphere: $1.055 \pm 0.054/1.059 \pm 0.051$, $P = 0.773$; Figure 4(a,c)).

Screening for cognitive impairment by MMSE revealed no significant group differences between the two time points of assessment (mean MMSE score in scan 1 controls/patients: $28.6 \pm 1.2/27.7 \pm 2.7$, $P = 0.222$; scan 2 controls/patients: $29.4 \pm 1.1/29.2 \pm 0.8$, $P = 0.689$; Table 1).

In a subgroup analysis, we compared the above-mentioned measures in patients with good collateralization status ($n = 11$) and those with poor collateralization status ($n = 5$). We found that the DC of iWSAs across scans was significantly lower ipsilateral to the stenosis in patients with poor collateralization (mean DC ipsilateral/contralateral to the stenosis: $0.549 \pm 0.049/0.642 \pm 0.025$; Figure 5), whereas patients with good collateralization did not show significant differences between both sides (mean DC ipsilateral/contralateral to the stenosis: $0.603 \pm 0.072/0.614 \pm 0.037$, $P = 0.504$). Both subgroups showed an increased DC of iWSA with the averaged WSA mask of controls in scan 2 compared to scan 1 (poor collaterals: mean DC in scan 1/2: $0.410 \pm 0.062/0.501 \pm 0.040$, $P = 0.024$; good collaterals: mean DC in scan 1/2: $0.448 \pm 0.033/0.517 \pm 0.045$, $P < 0.001$); however, no significant group difference was observed of DCs in both scans (scan 1/2: $P = 0.126/0.522$). Furthermore, patients with poor collateralization status had significantly lower MMSE results than those of controls tested at baseline (25.8 ± 3.8 vs. 28.6 ± 1.2), whereas no differences were found for the follow-up assessments (28.3 ± 0.58 vs. 29.4 ± 1.1, $P = 0.126$). Patients with good collateralization of the CoW did not show significantly different MMSE values to controls in both scans (baseline: $P = 0.938$, follow-up examination: $P = 0.780$).

Discussion

This study aimed to evaluate spatial variations of TTP-based iWSAs and associated hemodynamic changes in patients with high-grade asymptomatic ICAS after a revascularization procedure compared to healthy controls without intervention.

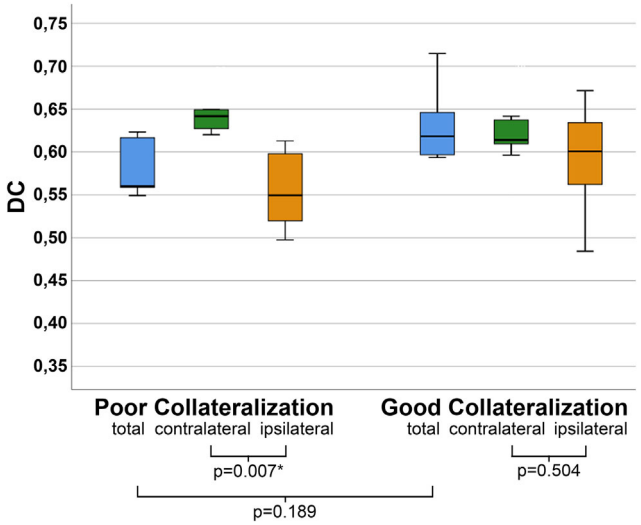

FIGURE 5: Increased spatial shift of individual watershed areas (iWSAs) in patients with poor collateralization of the Circle of Willis. In a subgroup analysis, patients with poor collateral status of the Circle of Willis showed a significantly lower spatial overlap of iWSA across scans on the side of the stenosis (median dice coefficient [DC] of iWSAs in the ipsilateral/contralateral hemisphere: 0.549/0.642, $P = 0.007$), whereas patients with good collateralization did not show significant side differences (median DC of iWSAs in the ipsilateral/contralateral hemisphere: 0.603/0.614, $P = 0.504$). This indicates that results in Figure 3(b) are driven by patients with reduced collateral flow, who may benefit more from invasive treatment. The boxes contain all single DC values between the first and third quartiles, the line inside marks the median, and the whiskers reach from minimum to maximum (not including outliers).

Our main finding was the shift of patients' iWSAs on the side of the stenosis after treatment, which was more pronounced in patients with a poor collateralization of the CoW. The spatial extent and location of iWSAs as well as the perfusion delay were normalized by the revascularization procedure. Moreover, cognitive screening revealed no significant group differences between baseline and follow-up examinations; however, patients with poor collateralization had significantly lower MMSE scores at baseline.

Normalization of IWSA

In a previous study, increased spatial variability of iWSAs in ICAS patients was observed.[14] Here, we demonstrated that this increased variability can be reversed by a revascularization procedure when comparing the preinterventional and postinterventional iWSAs. Specifically, patients' global iWSAs showed a decreased spatial congruency with a strong trend to statistical significance. This spatial incongruence was driven by a significantly reduced overlap of iWSAs on the side of the revascularized stenosis, indicating specific treatment-associated effects on iWSA location. After treatment of patients, iWSAs ipsilateral and contralateral to the stenosis were more similar to the controls' mean iWSAs, indicating a spatial normalization of iWSA location on both sides as a likely consequence of revascularization. The finding supports the notion that revascularization effects influence hemodynamics in both hemispheres, which can be explained by reduced vascular steal phenomena in the contralateral anterior circulation as described previously.[22] Another study demonstrated shifts of perfusion territories in hypercapnia, indicating a connection between flow and perfusion territories.[23] A normalization of vascular territories after intervention has been reported previously;[24] however, this did not show the spatial normalization of iWSAs in hemodynamically compromised patients by revascularization procedures.

In a subgroup analysis, we found that the shift of iWSAs ipsilateral to the revascularization treatment was more pronounced in patients with poor collateralization status of the CoW than in patients with good collateralization, however, we did not quantify collateral flow in our study. Zarrinkoob et al used 4D phase contrast MRI to evaluate blood flow in the CoW, stating the importance of the collateralization of the CoW to sustain blood supply to both hemispheres.[25] The stability of perfusion territories and iWSAs in patients with complete CoW therefore suggests a beneficial role of primary collaterals, which is in line with previous studies.[25,26]

Furthermore, it has been shown that collateral flow and the recruitment of additional secondary collaterals are associated with increased hemodynamic impairment.[27] The normalization of flow territories and WSAs after intervention may therefore be considered beneficial, since critical collateral flow is reduced, and hemodynamic decompensation might be less likely to happen. Derdeyn et al, however, did not report a correlation between misery perfusion and borderzone shifts as assessed by digital subtraction angiography.[28] This might be due to the lower spatial resolution of the projection radiography method compared to TTP maps, which could make it harder to detect subtle shifting of WSAs.

However, several studies have shown that hemodynamic impairments due to ICAS cannot be predicted based on the degree of stenosis and anatomy of the CoW alone.[25,29] The high variability and temporal shift of iWSAs underline the necessity to determine such areas individually to correctly identify borderzone ischemia. Accordingly, Hartkamp et al found that 10% of infarcts in patients with subacute stroke were misinterpreted as infarcts in a single perfusion territory but proved to be localized in the borderzone after evaluation of individual vascular territory maps derived from vessel-encoded arterial spin labeling (ASL).[30] Since watershed infarcts are considered signs of severe hemodynamic impairment in patients with ICAS,[10] reliable and rapid differentiation from ischemia of other origin is thus crucial when considering immediate revascularization therapy.[10]

Recovery of Hemodynamic Impairment

Apart from the spatial normalization of TTP-based iWSAs, the normalization of TTP itself as a marker of perfusion delay

due to reduced perfusion pressure in ICAS may be able to evaluate treatment success. We showed that pre-interventional rTTP values within iWSAs were higher in the ipsilateral hemisphere in patients than in the contralateral side. This finding is in line with other studies demonstrating that perfusion delay and hypoperfusion occur first in the ipsilateral iWSAs.[8,14] Specifically, we observed that the perfusion delay on the side of the stenosis was reduced after revascularization treatment and, thus, symmetrical bilateral perfusion was restored, supporting the notion that TTP changes can reliably track treatment effects on cerebral hemodynamics.

Effects on Cognition and WMHs

On a group level, the reversal of hemodynamic impairment did not translate into an improvement of cognition in patients as evaluated by MMSE. These findings are in line with a study by Schröder et al, who also demonstrated hemodynamic recovery but stable cognitive test scores after revascularization treatment in asymptomatic ICAS patients.[8] However, other studies with more advanced cognitive testing have revealed clear cognitive impairments in asymptomatic ICAS patients,[5,9] which may be missed by our clinical screening test.

Interestingly, a significantly reduced MMSE score was observed before intervention in patients with poor collateralization status as compared to healthy controls. This finding could explain variable findings and resulting controversy between studies investigating the effect of interventions on cognition in patients with ICAS.[31,32] The results of the present study indicated that only a subgroup of patients with poor collateralization of the CoW may actually benefit from an invasive procedure concerning cognitive improvements. However, because of the small number of patients in this subgroup ($n = 5$), this result must be taken with caution and certainly needs further investigation in larger patient cohorts.

Furthermore, WMHs have been linked to cognitive deficits[33] as well as chronic hypoperfusion[34] and are also used to monitor periprocedural ischemia.[35] Here, the Fazekas score of WMH remained stable between baseline and follow-up imaging in patients and controls, respectively. Only one patient presented with a new small lacunar lesion on the side of the stenosis after CAS. In the remaining patients, no new ischemic events were observed, indicating a minor periprocedural risk for lacunar infarcts in CAS, being in line with the literature.[35]

Reliability of IWSA Segmentation

The definition of iWSAs according to a segmentation approach based on DSC-derived TTP maps was reliably feasible in both groups as assessed by inter-rater comparisons, being in accordance with previously reported results.[14] In addition, the spatial congruency of iWSAs between scans was sufficiently high and symmetrical in the control group, which suggests the high reproducibility of this segmentation approach. Contrast-enhanced perfusion MRI is time-efficient and promising to determine hemodynamic compromise caused by ICAS and therefore widely integrated into clinical routines.[36] As our method is based on DSC-derived data, no additional measurements for iWSA determination are required, limiting the scan time for the patient. Contrast agent applications should be kept as low as possible according to the currently ongoing debate on gadolinium depositions.[37] Thus, we used a macrocyclic agent, which showed far less depositions. Furthermore, no associated symptoms of depositions have been revealed.[38]

Another approach for measuring cerebral perfusion delay is based on non-invasive ASL-derived arterial transit time maps,[39] which could also be used for iWSA segmentation. Compared with DSC, however, ASL has a lower signal-to-noise ratio, especially in white matter, where most parts of WSAs are located. This potentially limits the assessment of perfusion delay and thus iWSA definition in the brain's deep WM.[14] Alternatively, vascular territories can be determined by super-selective ASL[40] and thereby iWSAs can be defined where the different territories meet. Accordingly, WSAs located between branches of the deep and superficial supply system of the MCA cannot be delineated by this method.

Limitations

First, the number of patients and controls in this prospective study was small. However, despite this fact, the observed effects on iWSA location and hemodynamic changes were strong and revascularization effects could be clearly demonstrated. Second, although being statistically significant, side-differences of rTTP in iWSA on the affected vs. the unaffected side were relatively small while the standard deviation was comparably high ($1.103 \pm 0.083/1.050 \pm 0.069$). Also, normalization of TTP by the mean TTP of the contralateral MCA-territory did not change this. An explanation for this finding might be that the analysis of voxels within iWSA includes gray and white matter as well as cortical veins resulting in a higher TTP variability. Third, in our subgroup analysis in which the patients were divided into individuals with poor and good collateralization status, we only analyzed the role of potential collateral flow that the CoW configuration enables (i.e. we did not consider actual collateral flow or other collateral ways such as leptomeningeal and extra-intracranial collaterals). Fourth, the proposed segmentation approach is clearly operator dependent. However, in a previous publication, the reliability of this approach as well as agreement of iWSA location with the literature have been demonstrated.[14] In this prospective study, we could further validate the segmentation procedure as we demonstrated that the iWSA location of controls remained stable over time and showed high inter-rater agreement. Fifth, our age-matched

control group had significantly less comorbidities, such as hypertension and diabetes, and most likely less atherosclerotic changes. Thus, a control group consisting of non-revascularized patients with high-grade ICAS would be more suitable to reveal stenosis-specific impacts on cerebral hemodynamics and WSA location. To account for this limitation, we plan to include ICAS patients receiving only best medical treatment to further investigate influences of revascularization procedures on cerebral hemodynamics.

Conclusion

In our cohort of patients with asymptomatic unilateral high-grade ICAS, revascularization of the stenosis normalized the higher spatial variability of iWSAs as well as the impaired hemodynamics specifically in the ipsilateral hemisphere, whereas healthy controls presented stable iWSAs and perfusion delay over time. Data indicate that patients with poor collateral flow in particular may benefit from revascularization procedures in terms of spatial iWSA normalization and cognitive performance.

Acknowledgments

This work was supported by the German Research Foundation (grant no. PR 1039/6-1 to C.P.) and further supported by the Faculty of Medicine of the Technical University of Munich (grant to J.G.: KKF E12), by the Dr.-Ing. Leonhard Lorenz-Stiftung (grant to J.G.: 915/15, S.K.: 971/19), by the Friedrich-Ebert-Stiftung for S.K., and by a postdoc fellowship for J.G. of the German Academic Exchange Service (DAAD).

Conflict of Interests

The authors declared no potential conflicts of interest concerning the research, authorship, and/or publication of this article.

Authors Contribution

J.G., S.K., and C.P: Conzeptualization, Data Curation, Supervsision; J.G., S.K., C.P., and L.S.: Formal Analysis, Writing – Original Draft; N.S., M.K., HH.E., J.K., and C.Z.: Writing – Reviewing and Editing, Supervision. All authors approved the final version of the manuscript. Open Access funding enabled and organized by Projekt DEAL.

References

1. D'Amore C, Paciaroni M. Border-zone and watershed infarctions. Front Neurol Neurosci 2012;30:181-184.
2. Momjian-Mayor I, Baron J-C. The pathophysiology of watershed infarction in internal carotid artery disease: Review of cerebral perfusion studies. Stroke 2005;36(3):567-577.
3. Naylor AR. Endarterectomy versus stenting for stroke prevention. Stroke Vasc Neurol 2018;3(2):101-106.
4. Landgraff NC, Whitney SL, Rubinstein EN, Yonas H. Cognitive and physical performance in patients with asymptomatic carotid artery disease. J Neurol 2010;257(6):982-991.
5. Balestrini S, Perozzi C, Altamura C, et al. Severe carotid stenosis and impaired cerebral hemodynamics can influence cognitive deterioration. Neurology 2013;80(23):2145-2150.
6. Silvestrini M, Viticchi G, Falsetti L, et al. The role of carotid atherosclerosis in alzheimer's disease progression. J Alzheimers Dis 2011;25(4):719-726.
7. Kaczmarz S, Göttler J, Petr J, et al. Hemodynamic impairments within individual watershed areas in asymptomatic carotid artery stenosis by multimodal MRI. J Cereb Blood Flow Metab 2020;41(2):380-396.
8. Schröder J, Heinze M, Günther M, et al. Dynamics of brain perfusion and cognitive performance in revascularization of carotid artery stenosis. NeuroImage: Clinical 2019;22:101779.
9. Göttler J, Kaczmarz S, Nuttall R, et al. The stronger one-sided relative hypoperfusion, the more pronounced ipsilateral spatial attentional bias in patients with asymptomatic carotid stenosis. J Cereb Blood Flow Metab 2020;40(2):314-327.
10. Del Sette M, Eliasziw M, Streifler JY, Hachinski VC, Fox AJ, Barnett HJM. Internal borderzone infarction: A marker for severe stenosis in patients with symptomatic internal carotid artery disease. Stroke 2000;31(3):631-636.
11. Leblanc R, Lucas Yamamoto Y, Tyler JL, Diksic M, Hakim A. Borderzone ischemia. Ann Neurol 1987;22(6):707-713.
12. van Laar PJ, Hendrikse J, Klijn CJM, Kappelle LJ, van Osch MJP, van der Grond J. Symptomatic carotid artery occlusion: Flow territories of major brain-feeding arteries. Radiology 2007;242(2):526-534.
13. Richter V, Helle M, van Osch MJP, et al. Mr imaging of individual perfusion reorganization using superselective pseudocontinuous arterial spin-labeling in patients with complex extracranial steno-occlusive disease. AJNR Am J Neuroradiol 2017;38(4):703-711.
14. Kaczmarz S, Griese V, Preibisch C, et al. Increased variability of watershed areas in patients with high-grade carotid stenosis. Neuroradiology 2018;60(3):311-323.
15. Kawai N, Hatakeyama T, Okauchi M, et al. Cerebral blood flow and oxygen metabolism measurements using positron emission tomography on the first day after carotid artery stenting. J Stroke Cerebrovasc Dis 2014;23(2):55-64.
16. North American Symptomatic Carotid Endarterectomy Trial. Methods, patient characteristics, and progress. Stroke 1991;22(6):711-720.
17. Folstein MF, Folstein SE, McHugh PR. Mini-mental state: A practical method for grading the cognitive state of patients for the clinician. J Psychiatr Res 1975;12(3):189-198.
18. Welker K, Boxerman J, Kalnin A, et al. ASFNR recommendations for clinical performance of MR dynamic susceptibility contrast perfusion imaging of the brain. AJNR Am J Neuroradiol 2015;36(6):E41-E51.
19. Kluge A, Lukas M, Toth V, Pyka T, Zimmer C, Preibisch C. Analysis of three leakage-correction methods for DSC-based measurement of relative cerebral blood volume with respect to heterogeneity in human gliomas. Magn Reson Imaging 2016;34(4):410-421.
20. Penny W, Friston K, Ashburner J, et al. *Statistical parametric mapping: The analysis of functional brain images*. Amsterdam: Elsevier Science; 2011.
21. Fazekas F, Chawluk J, Alavi A, Hurtig H, Zimmerman R. MR signal abnormalities at 1.5 T in Alzheimer's dementia and normal aging. Am J Roentgenol 1987;149(2):351-356.
22. Sam K, Small E, Poublanc J, et al. Reduced contralateral cerebrovascular reserve in patients with unilateral steno-occlusive disease. Cerebrovasc Dis 2014;38(2):94-100.
23. Arteaga DF, Strother MK, Faraco CC, Davis LT, Scott AO, Donahue MJ. Cerebral blood flow territory instability in patients with atherosclerotic intracranial stenosis. J Magn Reson Imaging 2019;50(5):1441-1451.
24. Van Laar PJ, Hendrikse J, Mali WPTM, et al. Altered flow territories after carotid stenting and carotid endarterectomy. J Vasc Surg 2007;45(6):1155-1161.

25. Zarrinkoob L, Wåhlin A, Ambarki K, Birgander R, Eklund A, Malm J. Blood flow lateralization and collateral compensatory mechanisms in patients with carotid artery stenosis. Stroke 2019;50(5):1081-1088.

26. Henderson RD, Eliasziw M, Fox AJ, Rothwell PM, Barnett HJM. Angiographically defined collateral circulation and risk of stroke in patients with severe carotid artery stenosis. Stroke 2000;31(1):128-132.

27. Hartkamp NS, Petersen ET, Chappell MA, et al. Relationship between haemodynamic impairment and collateral blood flow in carotid artery disease. J Cereb Blood Flow Metab 2018;38(11):2021-2032.

28. Derdeyn CP, Shaibani A, Moran CJ, Cross DT, Grubb RL, Powers WJ. Lack of correlation between pattern of collateralization and misery perfusion in patients with carotid occlusion. Stroke 1999;30(5):1025-1032.

29. Powers WJ, Derdeyn CP, Fritsch SM, et al. Benign prognosis of never-symptomatic carotid occlusion. Neurology 2000;54(4):878-882.

30. Hartkamp NS, Hendrikse J, De Cocker LJL, de Borst GJ, Kappelle LJ, Bokkers RPH. Misinterpretation of ischaemic infarct location in relationship to the cerebrovascular territories. J Neurol Neurosurg Psychiatry 2016;87(10):1084-1090.

31. Chida K, Ogasawara K, Suga Y, et al. Postoperative cortical neural loss associated with cerebral hyperperfusion and cognitive impairment after carotid endarterectomy: ^{123} I-iomazenil spect study. Stroke 2009;40(2):448-453.

32. De Rango P, Caso V, Leys D, Paciaroni M, Lenti M, Cao P. The role of carotid artery stenting and carotid endarterectomy in cognitive performance: A systematic review. Stroke 2008;39(11):3116-3127.

33. Schmidt R, Petrovic K, Ropele S, Enzinger C, Fazekas F. Progression of leukoaraiosis and cognition. Stroke 2007;38(9):2619-2625.

34. ten Dam VH, van den Heuvel DMJ, de Craen AJM, et al. Decline in total cerebral blood flow is linked with increase in periventricular but not deep white matter hyperintensities. Radiology 2007;243(1):198-203.

35. Bonati LH, Jongen LM, Haller S, et al. New ischaemic brain lesions on MRI after stenting or endarterectomy for symptomatic carotid stenosis: A substudy of the international carotid stenting study (ICSS). Lancet Neurol 2010;9(4):353-362.

36. Marshall RS, Lazar RM, Liebeskind DS, et al. Carotid revascularization and medical management for asymptomatic carotid stenosis – Hemodynamics (CREST-H): Study design and rationale. Int J Stroke 2018;13(9):985-991.

37. Radbruch A. Are some agents less likely to deposit gadolinium in the brain? Magn Reson Imaging 2016;34(10):1351-1354.

38. Kanda T, Oba H, Toyoda K, Furui S. Macrocyclic gadolinium-based contrast agents do not cause hyperintensity in the dentate nucleus. Am J Neuroradiol 2016;37(5):E41-E41.

39. Hendrikse J, Petersen ET, van Laar PJ, Golay X. Cerebral border zones between distal end branches of intracranial arteries: Mr imaging. Radiology 2008;246(2):572-580.

40. Helle M, Rüfer S, van Osch MJP, et al. Superselective arterial spin labeling applied for flow territory mapping in various cerebrovascular diseases: Arterial spin labeling in cerebrovascular diseases. J Magn Reson Imaging 2013;38(2):496-503.